

The effect of high-velocity oxygen fuel, thermally sprayed WC–Co coatings on the high-cycle fatigue of aluminium alloy and steel

A. IBRAHIM, C. C. BERNDT

Department of Materials Science and Engineering, State University of New York at Stony Brook, Stony Brook, NY 11794, USA
E-mail: ibrahim@farmingdale.edu

Thermally sprayed WC–Co coatings are currently used in numerous contact wear applications in the aircraft, automotive and paper industries. High-cycle fatigue tests were performed at room temperature and 370°C on SAE 12L14 low-carbon steel and aluminium alloy 2024-T4 thermally sprayed with WC–17 wt% Co using the high-velocity oxygen fuel process. The fatigue life distributions of specimens in the polished, grit-blasted, peened and coated conditions are presented as a function of the probability of failure. Composite beam theory was applied to the coated beam to evaluate the stresses and elastic modulus. The stress–strain curves for the coated and uncoated specimens were used to evaluate the stiffness factor for the aluminium alloy and steel. It is concluded that (i) the coated specimens exhibited significantly high fatigue lives compared with the uncoated specimens, (ii) the mechanisms of deformation for the coated and uncoated aluminium alloy specimens are quite different and (iii) the elastic modulus of the coating plays a significant role in determining the fatigue strength of the coated component. © 1998 Kluwer Academic Publishers

1. Introduction

High-velocity oxygen fuel (HVOF) thermally sprayed WC–Co coatings on metallic substrates, particularly aluminium, have found wide use as wear- and corrosion-resistant coatings in many industrial applications. The HVOF process, which combines a relatively low thermal energy with a high kinetic energy, produces coatings with a high hardness, a low porosity and a high bond strength. The influence of the coating on the fatigue life of the base material has been the subject of several investigators; for instance thermally sprayed WC–Co exhibits favourable fatigue-resistant properties [1–5]. While most of these data have been devoted to establishing the S–N curve, less effort was given to understanding the deformation mechanism of the coating and the base material.

In order to evaluate the fatigue strength of a given material from a reliability viewpoint, the value of the stress versus life relation for prescribed failure probabilities (P–S–N relations) must be available [6]. For coated beams under applied bending moments or dynamic vibrations, the stiffness of the coated beam [6, 7] is an important factor in determining the strength of the component.

In this investigation, rotating bending high-cycle fatigue (HCF) of SAE 12L14 low-carbon steel and aluminium alloy 2024-T4 in the polished, grit-blasted and peened conditions, as well as coated with WC–Co, are investigated. The fatigue life distributions are presented as a function of the probability of failure.

The fracture mechanisms of the coated and uncoated specimens are also discussed on the basis of detailed macroscopic and metallographic analysis. Strain gauges were bonded to the test specimen to measure the elastic strain of the coated beam. Composite beam theory determined the stresses and elastic modulus of the coating. Finally, the stiffness factor was introduced to assess the resistance of the coated beam to bending stress.

2. Experimental procedure

The base materials used in this study were SAE 12L14 low-carbon steel and aluminium alloy 2024-T4. The mechanical properties of these materials are shown in Table I. The fatigue test specimen shown in Fig. 1 was prepared according to ASTM standard E466-82 [9].

The fatigue experiments were conducted at room temperature and 370°C under rotating bending ($R = -1$) at a loading frequency of 50 Hz. The surface of the specimen was prepared for coating by grit blasting with grade 24 alumina particles using a blasting pressure of 500 kPa. The specimens were coated with a WC–Co coating 0.200 mm thick using a HVOF system (DJ gun, Sulzer-Metco Inc., Westbury, NY). The elastic strains of coated and uncoated specimens were measured with strain gauges glued at the centre of the specimen surface. The fracture surfaces were characterized using optical and scanning electron microscopy (SEM).

TABLE I Mechanical properties of the substrate materials [8]

Material	Yield point σ_y (MPa)	Tensile strength σ_U (MPa)	Elastic modulus E (GPa)	Elongation to fracture δ (%)	Vickers hardness (HV)
SAE 12L14	540	630	204	10	195
Al alloy 2024-T4	375	470	75	20	137

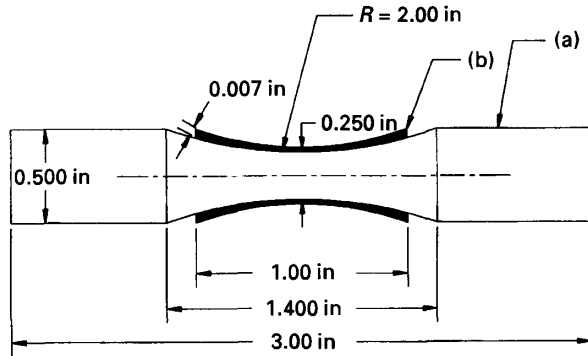


Figure 1 (a) Specimen configuration according to [8]. The placement of the coating (b) is indicated by the thick solid line.

3. Results and discussion

3.1. Fatigue life distributions

HCF tests were conducted at stress amplitudes of 530 MPa and 355 MPa for steel and aluminium alloy specimens, respectively. The sample size was nine for each material condition. The failure probability [10, 11], P_f , corresponding to the order number i is given by

$$P_f = \frac{i}{n + 1}$$

where n is the sample size.

Fig. 2 shows the probability, P_f , of failure, as a function of number, N , of cycles to failure for the coated and uncoated steel specimens at room temperature and 370°C. The results indicate that grit blasting slightly decreases the fatigue strength of the steel. At room temperature the fatigue strength of the steel is significantly improved by the WC-Co coating, i.e. the mean N_f changes from 12833 to 660688 (Table II). However, at 370°C the fatigue life of the coated specimen decreases, i.e. the mean N_f decreases from 660688 to 35688.

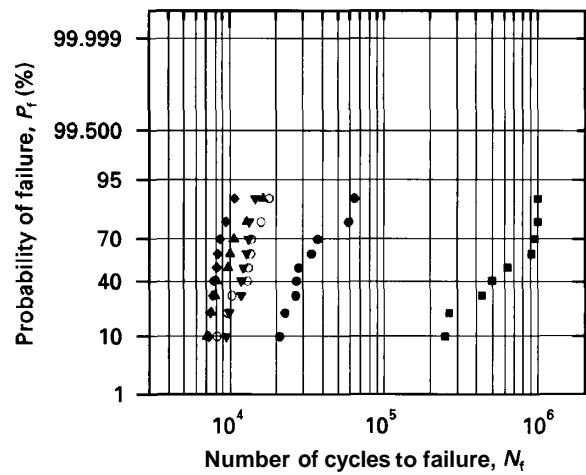


Figure 2 Fatigue life distributions of SAE 12L14 steel (log normal; $S = 530$ MPa). (○), as-polished, room temperature; (◆), as-polished, $T = 370^\circ\text{C}$; (▲), grit-blasted, room temperature; (△), as-grit-blasted, $T = 370^\circ\text{C}$; (■), as-coated with WC-Co, room temperature; (●), as-coated with WC-Co, $T = 370^\circ\text{C}$.

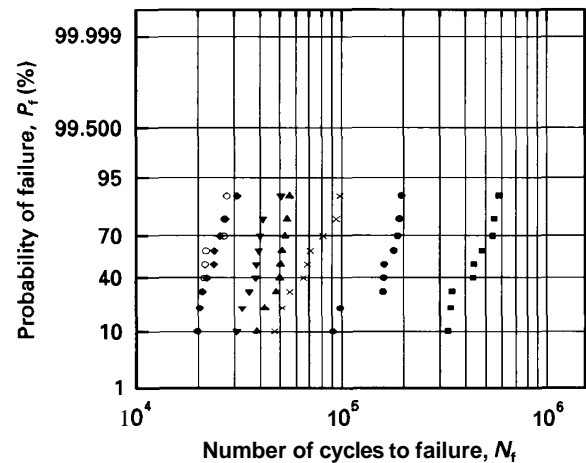


Figure 3 Fatigue life distributions of aluminium alloy 2024-T4 (log normal; $S = 355$ MPa). (○), as-polished, room temperature; (◆), as-polished $T = 370^\circ\text{C}$; (▲), grit-blasted, room temperature; (△), as-grit-blasted, $T = 370^\circ\text{C}$; (×), as-peened, room temperature; (■), as-coated with WC-Co, room temperature; (●), as-coated with WC-Co, $T = 370^\circ\text{C}$.

Fig. 3 and Table III show similar effects for aluminium alloy 2024-T4. These results indicate that grit blasting and shot peening increase the fatigue strength of the substrate material [2]. Moreover, the fatigue strength of aluminium alloy is improved by the WC-Co coating. As shown in Fig. 3, the high temperature

TABLE II Statistics of the fatigue life of SAE 12L14 steel where σ is the standard deviation, CV is the coefficient of variation and $N/N_{P(RT)}$ is the fatigue life N compared with the as-polished (room-temperature) base level $N_{P(RT)}$

Number	Specimen condition	Number of cycles to failure, N_f			σ	CV (%)	$N/N_{P(RT)}$
		Minimum	Mean	Maximum			
1	Polished (room temperature)	8200	12833	18000	3120	24	1
2	Polished (370°C)	7200	8366	10700	1098	13	0.65
3	Grit blasted (room temperature)	9400	12088	14600	1667	14	0.94
4	Grit blasted (370°C)	7000	10011	16400	3003	30	0.78
5	Coated, WC-Co (room temperature)	248700	660688	1000100	313015	47	51.48
6	Coated, WC-Co (370°C)	21000	35688	64800	15868	44	2.78

TABLE III Statistics of the fatigue life of aluminium alloy 2024-T4 where σ is the standard deviation, CV is the coefficient of variation and $N/N_{P(RT)}$ is the fatigue life N compared with the as-polished (room temperature) base level $N_{P(RT)}$

Number	Specimen condition	Number of cycles to failure, N_f			σ	CV (%)	$N/N_{P(RT)}$
		Minimum	Mean	Maximum			
1	Polished (room temperature)	19700	22977	27600	3119	14	1
2	Polished (370°C)	19800	23822	31000	3624	15	1.04
3	Grit blasted (room temperature)	30600	38422	50500	5706	15	1.67
4	Grit blasted (370°C)	38200	49055	55600	5632	11	2.13
5	As-peened (room temperature)	46700	70088	98300	18213	26	3.05
6	Coated, WC-Co (room temperature)	327300	448466	581900	97546	22	19.52
7	Coated, WC-Co (370°C)	90400	158445	195600	38683	24	6.90

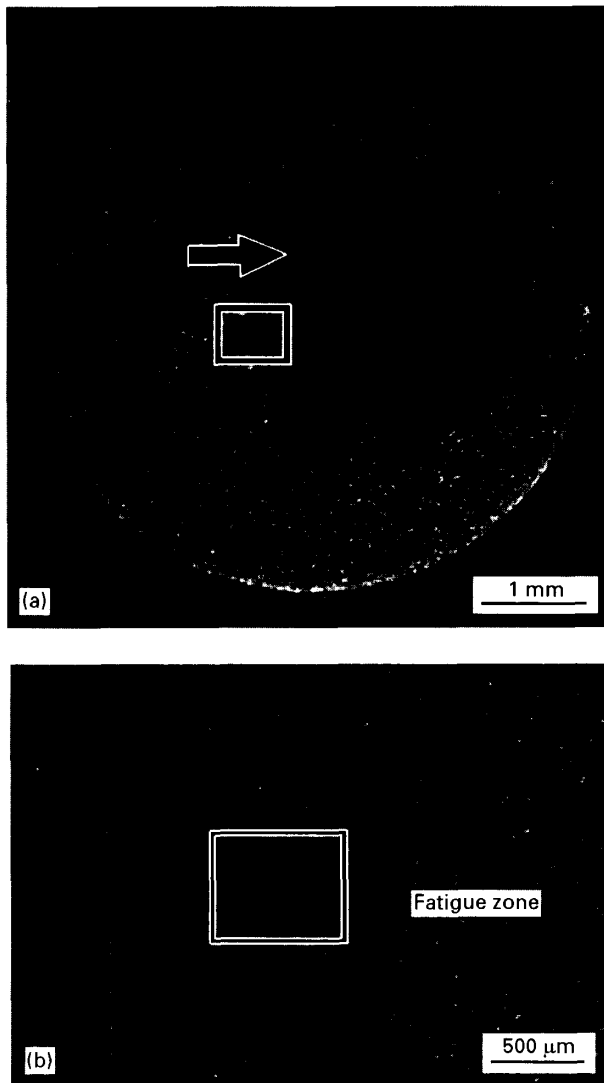


Figure 4 (a) Fractograph of the fracture surface of an SAE 12L14 specimen coated with WC-Co that failed at $\sigma = 530$ MPa, $N = 1000$ 100 cycles and $T = 23^\circ\text{C}$. (b) A SEM fractograph showing the transition zone between ductile and brittle fracture for the specimen in (a).

diminishes the fatigue strength of the WC-Co-coated specimen.

3.2. Fractography

The fracture surface of a coated steel specimen is shown in Fig. 4a. The fracture surface indicates that

fatigue originated at the centre of the dark area [12] indicated by the arrow. Fig. 4b shows a progressive crack separating the dark area (fatigue origin) from the rest of the substrate material. Examination of this area revealed that microvoids and dimples have grown and joined to form cracks that grew radially outwards [13, 14]. At 370°C the dark area (fatigue origin) was larger, thereby indicating higher deformation.

Visual and macroscopic examination of the coated aluminium alloy fracture surface indicate that the fracture surface in Fig. 5a consists of two distinct zones, indicated by A and B. Fig. 5b shows the transition between the two zones. Zone A shows cracks and significant plastic deformation, both characteristics of ductile fracture that started at the periphery of the substrate and propagated towards the centre of the material. Zone B exhibits cleavage features that are characteristics of brittle fracture. Continuous monitoring of the specimen during the test revealed that no coating peeled from the specimen in the early stage of the loading. However, at the final stage of loading of each test, a small section of the coating delaminated from the surface prior to complete failure. In a typical test the experiment was interrupted to examine the failure location (Fig. 6a) and revealed that the substrate material was extensively deformed (Fig. 6b). Therefore, the mechanism of coating failure is extensive deformation followed by progressive cracking at the surface of the aluminium alloy substrate, giving rise to a segment of the coating which was essentially standing free without support. At 370°C the number of such cracks increased and formed an array along the upper half of the specimen.

Fracture surfaces of the polished and grit-blasted aluminium alloy specimens are shown in Figs 7 and 8. The polished specimen plastically deformed extensively compared with the as-coated specimen (Fig 5). Thus, the coating has significantly reduced the rate of deformation and consequently the fatigue life is increased. As shown in Fig. 8, the grit-blasting procedure lead to the formation of a protective layer on the periphery of the specimen. This layer is the outermost layer that was work hardened due to the compressive residual stress during grit blasting. Therefore, fatigue nucleation was initiated just below the hardened layer; consequently, the rate of the fatigue process decreased and the fatigue life increased.

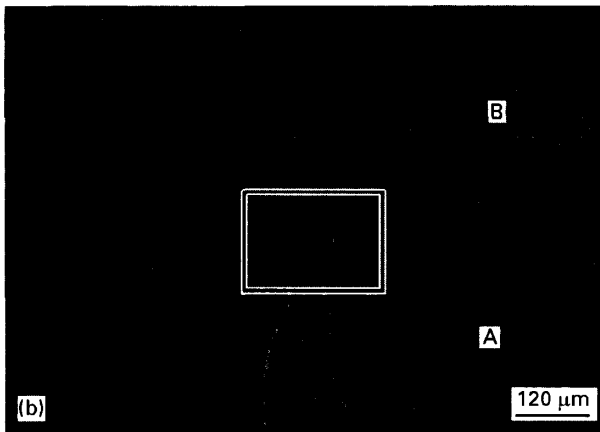
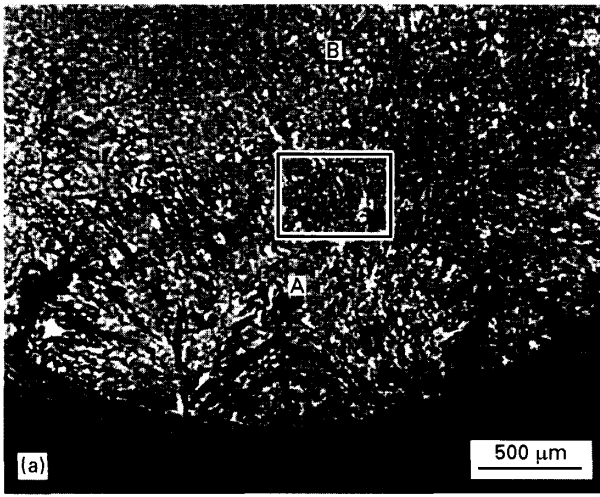


Figure 5 (a) Fractograph of the fracture surface of an aluminium alloy of 2024-T4 specimen coated with WC-Co that failed at $\sigma = 355$ MPa, $N = 327\,300$ cycles and $T = 23^\circ\text{C}$. (b) A SEM fractograph showing the transition zone between ductile and brittle fracture for the specimen in (a).

3.3. Bending stresses of coated beams

HVOF WC-Co coatings sprayed onto cylindrical specimens exhibit high adhesion strength and high density. In addition the thickness of the coating is usually small compared with the substrate. Therefore, the coated specimen behaves like a homogeneous composite material and may be analysed by the same bending theory used for ordinary beams, provided that the assumption that plane cross-sections before bending remain plane after bending. The normal stress, σ_x , acting on the cross-section as a result of bending moment, M , can be obtained from the strains, ϵ_x , using the stress-strain relationships for the materials. Denoting the modulus of elasticity for the substrate as E_S and of the elasticity modulus of the coating as E_C and also assuming that $E_C > E_S$, we obtain the stress diagram in Fig. 9.

The normal stresses, σ_x , at distance y from the x axis in the coating and substrate, are given by the following equations

$$\sigma_C = -E_C \kappa y \quad \sigma_S = -E_S \kappa y \quad (1)$$

Where κ is the curvature and y is the distance from the neutral axis.

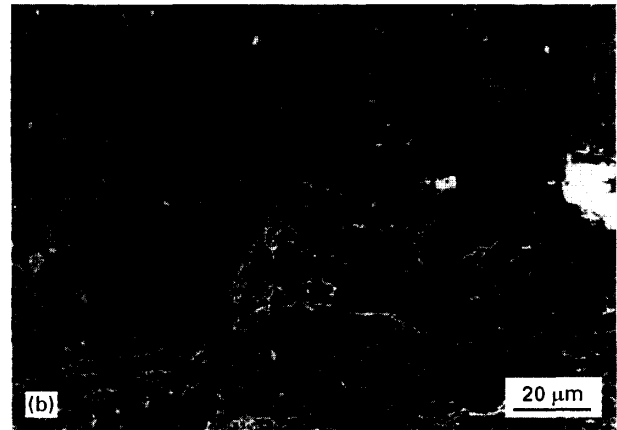
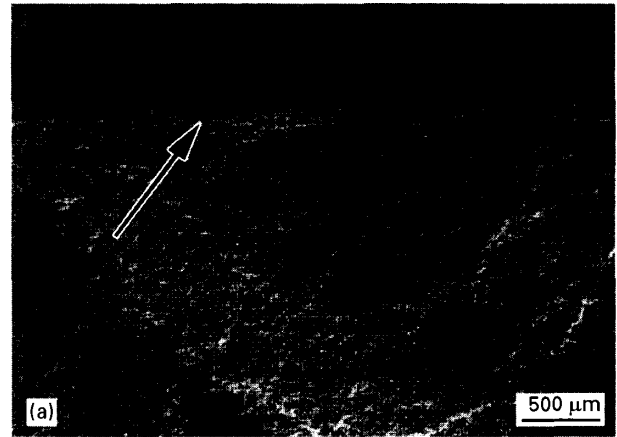


Figure 6 Fractograph of an aluminium alloy 2024-T4 specimen coated with WC-Co. (a) The dark area is the origin of failure and the white area is the location, where the coating is peeled off as a result of substrate damage. (b) A close-up picture for the dark area in (a). The test stopped at $\sigma = 355$ MPa and $N = 534\,800$ cycles.

The relationship between the bending moment, M , and the stress in the beam is as follows

$$M = \int \sigma_x y \, dA$$

Applying this formula for coated beams gives

$$\begin{aligned} M &= \int \sigma_S y \, dA + \int \sigma_C y \, dA \\ M &= -\kappa E_S \int y^2 \, dA - \kappa E_C \int y^2 \, dA \quad (2) \\ M &= -\kappa (E_S I_S + E_C I_C) \end{aligned}$$

Equation 2 can be solved for the curvature, κ

$$\kappa = -\frac{M}{E_S I_S + E_C I_C} \quad (3)$$

The stresses in the coated beams are obtained by substituting the expressions for curvature into the expressions for σ_C and σ_S (Equation 1)

$$\sigma_S = \frac{MyE_S}{E_S I_S + E_C I_C}, \quad \sigma_C = \frac{MyE_C}{E_S I_S + E_C I_C} \quad (4)$$

These expressions are the flexure formulae for coated beams. The relationship between the longitudinal

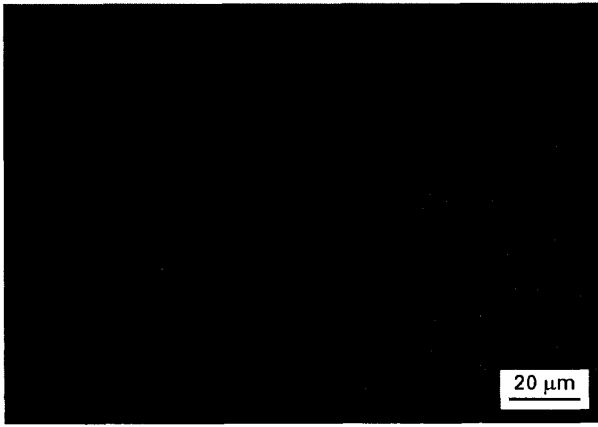


Figure 7 A SEM fractograph of the fracture surface of an aluminium alloy of 2024-T4 specimen that failed at $\sigma = 270$ MPa, $N = 176900$ cycles and $T = 23^\circ\text{C}$.

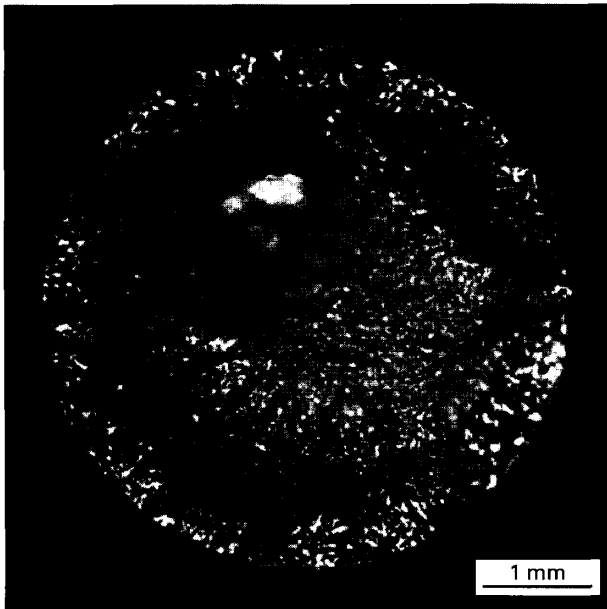


Figure 8 Fractograph of the fracture surface of a grit-blasted aluminium alloy 2024-T4 specimen that failed at $\sigma = 270$ MPa, $N = 277000$ cycles and $T = 23^\circ\text{C}$.

normal strain and the curvature is

$$\varepsilon_x = -\kappa y \quad (5)$$

Equations 3 and 5 can be used to determine the modulus of elasticity of the coating.

3.4. Stress–strain curves

Strain gauges were glued to the surface of the specimen and the stress–strain curves determined (Fig. 10); the coating–substrate composite exhibits a greater elastic modulus than the substrate material alone.

3.5. Stiffness factor, $(EI)_C/EI$

The elastic moduli derived from the stress–strain curves shown in Fig. 10 can be used to evaluate the stiffness factor, $(EI)_C/EI$, i.e. the ratio of the stiffness of an as-coated specimen to the stiffness of an uncoated specimen. Denoting the stiffnesses of the uncoated

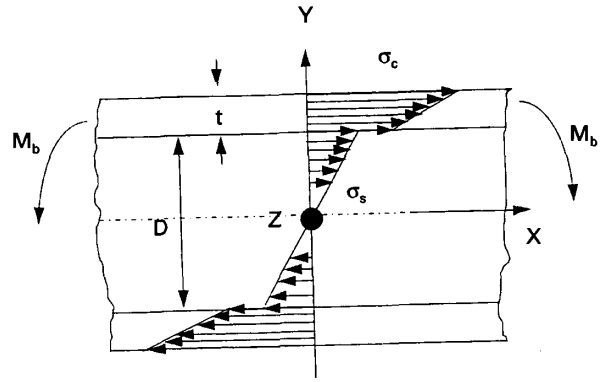


Figure 9 Variations in the bending stresses in the WC–Co coating and the substrate material.

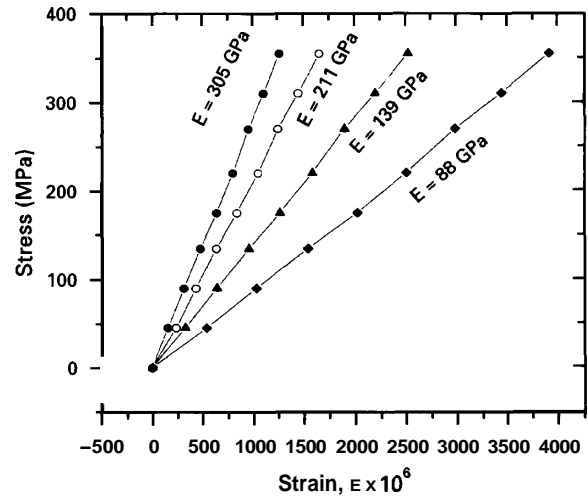


Figure 10 Stress–strain diagram for aluminium alloy 2024-T4 (\blacklozenge), as-polished; (A), as-coated with WC–Co) and SAE 12L14 steel (\circ), as-polished; (\bullet), as-coated with WC–Co).

aluminium alloy and steel specimens as $(EI)_A$, and $(EI)_S$, respectively, and the stiffnesses of the coated specimens as $(EI)_{AC}$ and $(EI)_{SC}$, then the stiffness factors, SF, for each material are

$$SF_A = \frac{(EI)_{AC}}{(EI)_A} = 1.95 \pm 0.12$$

$$SF_S = \frac{(EI)_{SC}}{(EI)_S} = 1.80 \pm 0.09$$

To evaluate the effect of grit blasting on the stiffness of the specimen, the elastic moduli of grit-blasted aluminium alloy and steel specimens were measured using strain gauges. The stiffness factors for grit-blasted aluminium alloy and steel are $SF_{GBA} = 1.20 \pm 0.07$ and $SF_{GBS} = 0.96 \pm 0.05$, respectively. This result indicates that grit blasting is more effective for the case of aluminium alloy. This also agrees well with the fatigue life data, i.e. N_f for polished material is less than N_f for grit-blasted material. Quantitative analysis of the SF factor and N_f ratio for aluminium alloy and steel is given in Table IV.

Residual stresses can influence the stiffness of the coated specimen, particularly flat specimens. The degree of influence depends on the magnitude and direction of the residual stresses. The stiffness factor, SF,

TABLE IV N_f ratios and SF factors for aluminium alloy and steel

Material	Elastic modulus ^a E (GPa)	Stiffness factor, SF		N_{fC}/N_{fP}	
		SF_{GR}	SF_C	Room temperature	370°C
SAE 12L14	211	0.96 ± 0.05	1.80 ± 0.09	51.48	2.78
Al alloy 2024-T4	88	1.20 ± 0.07	1.95 ± 0.12	19.52	6.90

^a Experimental value.

can, therefore, be used as a measure of the effectiveness of the coating in strengthening the coated component.

4. Conclusions

The influence of the HVOF sprayed WC–Co coating on the HCF of steel and aluminium alloy substrates can be summarized as follows.

1. Coatings of WC–Co improve the fatigue strength of steel and aluminium alloy.

2. At room temperature the fracture mechanism of coated aluminium alloy can be described as (i) initiation of cracks at the periphery of the substrate due to fatigue, (ii) propagation of the cracks towards the centre as well as to the circumference of the substrate, (iii) delamination of the coating at highly deformed locations on the periphery of the substrate, (iv) propagation of circumferential cracks through the coating and (v) final fracture of the specimen.

3. At room temperature the fracture mechanism of the coated steel can be described as (i) initiation of microvoids in the interior of the cross-section, (ii) coalescence of microvoids, (iii) formation of continuous cracks, (iv) growth of the cracks towards the free surface and (v) final fracture of the specimen.

4. At 370°C the fatigue resistance of WC–Co is significantly reduced, i.e. the mean N_f for steel decreases from 660688 to 35688 and the mean N_f for aluminium alloy decreases from 448466 to 158455.

5. Cylindrical specimens sprayed with WC–Co using the HVOF process behave like a homogeneous composite material, as the adhesion strength and density are high and the thickness of the coating is usually small compared with the substrate. Therefore, composite beam theory can be used to evaluate the stresses and elastic modulus of the coated beam.

6. The stiffness factor, $(EI)_C/EI$, can be used to measure the effectiveness of the coating. In the case of steel and aluminium alloy coated with WC–Co, these

ratios were 1.80 ± 0.09 and 1.95 ± 0.12 , respectively, and this indicates an increase in the fatigue strength of the coated specimens.

Acknowledgement

One of the authors (CCB) acknowledges support from DMR9632570.

References

1. A. TIPTON, in "Thermal spray science and technology", edited by C. C. Berndt and S. Sampath (ASM Int., Materials Park, OH, 1995) pp. 463–468.
2. H. STEFFENS, J. WILDEN, K. NASSENSTEIN and S. MOBUS, in "Thermal spray science and technology", edited by C. C. Berndt and S. Sampath (ASM Int., Materials Park, OH, 1995) pp. 469–474.
3. O. C. BRANDT, *J. Therm. Spray. Technol.* **4** (1995) 145.
4. T. SHIRAIISHI, H. OGIYAMA and H. TSUKUDA, in Proceedings of ITSC, Kobe, 1995 (1995) pp. 845–850.
5. J. HWANG, T. OGAWA and K. TOKAJI, in Proceedings of ITSC, Kobe, 1995 (1995) pp. 767–772.
6. T. TANAKA, S. NISHIJIMA and M. ICHIKAWA, "Statistical research on fatigue" (Elsevier, Amsterdam, 1987).
7. J. GERE and S. TIMOSHENKO, "Mechanics of materials" (PWS–Kent, Boston, MA, 1990).
8. "Metals handbook", Vol. 1 (ASM Int., Materials Park, OH, 1990).
9. ASTM Standard E 466-82, in "1992 annual book of ASTM standards", Vol. 03.01 (American Society for Testing and Materials, Philadelphia, PA, 1993) pp. 564–567.
10. C. K. LIN and C. C. BERNDT, *J. Mater. Sci.* **30** (1995) 111.
11. A. M. HASHEM and I. H. ALY, *Int. J. Fatigue*, **16** (1994) 321.
12. N. FROST, K. MARSH and L. POOK, "Metal fatigue" (Oxford University Press, Oxford, 1974).
13. R. KOTERAZAWA, R. EBARA and S. NISHIDA, "Fractography" (Elsevier, Amsterdam, 1990).
14. "Metals handbook", Vol. 10 (ASM Int., Metals Park, OH, 1975).

Received 27 January

and accepted 12 November 1997